

1 Gaseous elemental mercury (GEM) fluxes over canopy of two typical 2 subtropical forests in south China

3 Qian Yu¹, Yao Luo¹, Shuxiao Wang^{1,2}, Zhiqi Wang¹, Jiming Hao^{1,2}, Lei Duan^{1,2}

4 ¹State Key Laboratory of Environmental Simulation and Pollution Control, School of Environment, Tsinghua University,
5 Beijing 100084, China.

6 ²Collaborative Innovation Centre for Regional Environmental Quality, Tsinghua University, Beijing 100084, China.

7 *Correspondence to:* Lei Duan (lduan@tsinghua.edu.cn)

8 **Abstract.** Mercury (Hg) exchange between forests and the atmosphere plays an important role in global Hg cycling. The
9 present estimate of global emission of Hg from natural source has large uncertainty partly due to the lack of chronical and
10 valid field data, particularly for terrestrial surfaces in China, the most important contributor to global atmospheric Hg. In this
11 study, micrometeorological method (MM) was used to continuously observe gaseous elemental mercury (GEM) fluxes over
12 forest canopy at a clean-mildly polluted site (Qianyanzhou, QYZ) and a contaminated-moderately polluted site (Huitong, HT,
13 near a large Hg mine) in subtropical south China for a full year from January to December in 2014. The GEM flux
14 measurements over forest canopy in QYZ and HT showed net emission with annual average values of 6.67 and 1.210.30 ng
15 m⁻² h⁻¹ respectively. Daily variations of GEM fluxes showed an increasing emission with the increasing air temperature and
16 solar radiation in the daytime to a peak at 1:00 pm, and decreasing emission thereafter, even as a GEM sink or balance at night.
17 High temperature and low air Hg concentration resulted in the high Hg emission in summer. Low temperature in winter and
18 Hg absorption by plant in spring resulted in low Hg emission, or even adsorption in the two seasons. GEM fluxes were
19 positively correlated with air temperature, soil temperature, wind speed, and solar radiation while negatively correlated with
20 air humidity and atmospheric GEM concentration. The lower emission fluxes of GEM at the contaminated-moderately polluted
21 site (HT) when comparing with that in the clean-mildly polluted site (QYZ), may result from a much higher adsorption fluxes
22 at night in spite of a similar or higher emission fluxes during daytime. It testified that the higher atmospheric GEM
23 concentration at HT restricted the forest GEM emission. Great attention should be paid on forest as a critical increasing Hg
24 emission source with the decreasing atmospheric GEM concentration in polluted area because of the Hg emission abatement
25 in the future.

26 1 Introduction

27 Mercury (Hg) is a world-wide concerned environmental contaminant due to its cyclic transport between air, water, soil, and
28 the biosphere, and its tendency to bioaccumulate in the environment as neurotoxic mono-methylated compounds(CH₃Hg-)
29 (Driscoll et al., 2013), which can cause damage to the environment and human health (Lindqvist et al., 1991). Atmospheric
30 Hg exists in three different forms with different chemical and physical properties: gaseous elemental mercury (GEM, Hg⁰),

31 gaseous oxidized mercury (GOM, Hg²⁺), and particulate-bound mercury (PBM, Hg^p). Because of its mild reactivity, high
32 volatility, and low dry deposition velocity and water solubility, GEM is the most abundant form of Hg in the atmosphere
33 (Gustin and Jaffe, 2010; Holmes et al., 2010), and can long-distance transport due to the long residence time (0.5~2 yr)
34 (Schroeder et al., 1998).

35 Hg emission flux from anthropogenic sources has been quantified with reasonable consistency from 1900 to 2500 t yr⁻¹ (Streets
36 et al., 2009; Streets et al., 2011; Zhang et al., 2015; Zhang et al., 2016). However, the present estimates of natural Hg emission
37 from waters, soils, and vegetation are poorly constrained and have large uncertainties, with the values larger than anthropogenic
38 emission (e.g., 2000 t yr⁻¹, Lindqvist et al., 1991; 5207 t yr⁻¹, Pirrone et al., 2010; 4080~6950 t yr⁻¹, UNEP, 2013; 4380~6630
39 t yr⁻¹ Zhu et al., 2016). The reliable quantification of natural Hg source, specifically GEM exchange between terrestrial
40 ecosystem and the atmosphere would contribute to the understanding of global and regional Hg cycling budgets (Pirrone et al.,
41 2010; Wang et al., 2014b; Song et al., 2015).

42 As a dominant ecosystem on the Earth, forest is generally regarded as an active pool of Hg (Lindberg et al., 2007; Ericksen et
43 al., 2003; Sigler et al., 2009). Hg in the forest ecosystem is derived primarily from atmospheric deposition (Grigal, 2003), and
44 foliar uptake of GEM has been recognized as a principal pathway for atmospheric Hg to enter terrestrial ecosystems (Frescholtz
45 et al., 2003; Niu et al., 2011; Obrist, 2007). Accumulated Hg in foliage is transferred to soil reservoirs via plant detritus (St
46 Louis et al., 2001) or may partially be released back into the atmosphere (Bash and Miller, 2009). In addition, Hg may enter
47 the foliage by recycling processes, releasing GEM from underlying soil surfaces (Millhollen et al., 2006b). Soil-air GEM
48 exchange is controlled by numerous factors including physicochemical properties of soil substrate and abiotic/biotic processes
49 in the soil, meteorological conditions, and atmospheric composition (Bahlmann et al., 2006; Carpi and Lindberg, 1997; Engle
50 et al., 2005; Fritsche et al., 2008a; Gustin, 2011; Rinklebe et al., 2010; Mauclair et al., 2008; Zhang et al., 2008). The majority
51 of reported GEM flux measurements over terrestrial soils indicated net emission in warmer seasons and near-zero fluxes at
52 cold temperatures (Sommar et al., 2013). There are ongoing debates regarding whether or not forest is a sink or a source of
53 GEM because the forest/air exchange flux is the sum of vegetation and soil exchange flux, depending on not only atmospheric
54 concentration and meteorological conditions, but also plant community composition (Bash and Miller, 2009; Converse et al.,
55 2010) over shorter or longer periods.

56 China is currently the world's top emitter of anthropogenic Hg with a value of 538t in 2010 (Zhang et al., 2015) and 530t in
57 2014 (Wu et al., 2016), which resulted in an elevated Hg deposition to terrestrial ecosystem and thus Hg accumulate in land
58 surface. Given the forest is likely to have large GEM re-emission of legacy Hg stored through old-deposition, it is important
59 to know the role of forests in China in global Hg transport and cycle. However, there are far fewer long-time studies of forest
60 GEM exchange flux in China, especially for the subtropical forest, which is unique in the world. In this study, directly
61 measurements of net exchange of GEM over canopy of subtropical forests was conducted at a relatively ~~clean~~-mildly polluted
62 site and a ~~relatively-moderately~~ polluted site impacted by an adjacent Hg mine in south China. The objective of this study is
63 to quantify the natural Hg emission from the typical forest ecosystems, and analyse its influencing factors.

64 **2 Materials and methods**

65 **2.1 Site description**

66 This study was conducted at Qianyanzhou (QYZ) and Huitong (HT) experimental stations managed by the Chinese Academy
67 of Sciences (CAS) and Central South University of Forestry and Technology (CSUFT), respectively. The QYZ station
68 (115°04'E, 26°45'N) is located in Taihe county, Jiangxi province (Figure1, Table 1), surrounded by farmland, with no
69 obviously anthropogenic mercury sources such as coal-fired power plants and metal smelters in 25 km around. The HT station
70 (109°45'E, 26°50'N) is located in Huitong county, Hunan province, about 100 km away from the Wanshan Mercury Mine (WS),
71 which used to be the largest mercury mine in China. The two study sites have the similar climate condition. The dominant soil
72 and vegetation types (Table 1) are widely distributed in subtropical monsoon climate zone in south China. The subtropical
73 evergreen coniferous forests have fairly thick canopy, even in winter.

74 **2.2 Flux monitoring**

75 The continuous monitoring system of GEM vertical concentration gradient over forest canopy included a Hg detector, two
76 series of intake pipeline, and an automatically controlled valve system (Figure 2). The air sampling head and pipeline was
77 arranged on the flux tower, while the valve system and mercury detector was set in the cabin near the flux tower. Two automatic
78 GEM analyzers, model 2537X and 2537B (Tekran Instruments Inc.), with the same working principle and the detection limit
79 (less than 0.1 ng m⁻³, Gustin et al., 2013), were used at QYZ and HT site respectively. Air intakes were placed at two different
80 heights (25 and 35 m of the 41 m-high flux tower at QYZ site; 22.5 and 30.5 m on the 33m-high flux tower at HT site).
81 Considering the extremely large disturbance of temperature and wind speed over forest canopy, especially close to the canopy,
82 the lower air intake should be set at least half canopy height (Table 1) above the canopy to ensure the stability of the results
83 (Lindberg et al., 1998). Besides, all the air intakes would be fixed out of the tower body more than 1 m to avoid the influence
84 of the tower. Passing a particulate filter membrane (0.2 μm) and a soda lime adsorption tank just after the intake to remove
85 particulate matters, organic matters and acid gases, the in-gas from each height was pumped through a separated pipe ($\Phi =$
86 0.25 in) to the same Hg detector in turn, controlled by two 3-way electromagnetic valves manipulated by a time relay. The
87 electromagnetic valve switched once every 10 min, i.e., the measuring time of the gas from each height was 10 min, and it
88 took 20 min for a whole measuring cycle. The design of the system including the pump ensured the continuing air flow at the
89 same velocity in the two pipeline, whether the gas was sent to detect or no, to avoid the retention of air of the last cycle in the
90 pipeline. The pipeline, air intakes and valves are made of Teflon to avoid the adsorption of Hg.

91 Meteorological parameters were also measured continuously by setting air temperature, humidity and wind speed sensors at
92 the two heights (same to the air intakes), the solar radiation sensor and rainfall monitor at the higher height, and soil temperature
93 and moisture sensors at 5 cm depth in soil about 20 m away from the flux tower. All the sensors adopted international advanced
94 and reliable model (Table S1). All kinds of meteorological data were output by the data acquisition system (CR1000, Campbell
95 Scientific Inc., USA) every five minutes.

96 The observations of GEM concentration gradient and meteorological parameters lasted for one year at both sites from January
97 to December in 2014.

98 **2.3 GEM flux calculation**

99 The dynamic Flux Chamber (DFCs) and micrometeorological techniques (MM) are the mostly widely applied approaches for
100 surface/atmosphere GEM flux quantification (Zhu et al., 2016). The MM methods, including of direct flux measurement
101 method (the relaxed eddy accumulation method, REA) and the gradient methods (further divided to the aerodynamic gradient
102 method, AGM, and the modified Bowen-ratio method, MBR), were usually defined to measure the GEM flux over forest
103 canopy with the advantages of no interference on measuring interface and high capability of chronical measuring large scale
104 fluxes. The AGM method, which has been used over grasslands, agricultural lands, salt marshes, landfills, and snow surface
105 (Lee et al., 2000; Kim et al., 2001; Kim et al., 2003; Cobbett et al., 2007; Cobbett and Van Heyst, 2007; Fritsche et al., 2008b;
106 Fritsche et al., 2008c; Baya and Van Heyst, 2010), was used in this study. According to the AGM method, the GEM fluxes
107 (F , $\text{ng}\cdot\text{m}^{-2}\cdot\text{s}^{-1}$) over forest canopy was calculated on the basis of the measurement of the vertical concentration gradient by
108 using the following Eq. (1):

$$109 \quad F = K \frac{\partial c}{\partial z}, \quad (1)$$

110 Where K is turbulent transfer coefficient ($\text{m}^2 \text{s}^{-1}$), c is GEM concentration in the atmosphere (ng m^{-3}), and z is the vertical
111 height (m). Here, the GEM concentrations difference between the two air intakes divided by the height difference was assumed
112 to be the vertical gradient of atmospheric GEM concentration. Since the automatic GEM analyser switches between two gold
113 tubes and gets a value every 5 min, the two concentrations were averaged in each 10 min (matched to the single height sampling
114 interval by adjusting the time relay) to avoid possible bias caused by different gold tubes. The 20min variations of GEM
115 concentration at certain height were between -2% to 2% and -4% to 4% (95% confidence interval) at QYZ and HT sites
116 respectively. Thus, the GEM concentration was in a semi-steady state during the sampling interval. The GEM concentration
117 differences were calculated as the average concentrations at the higher height minus the two adjacent average concentrations
118 at the lower sampling height (all in 10 min interval). Thus, the vertical gradient of air GEM concentration can be gained every
119 10 min. Turbulent transfer coefficient K was calculated through specific steps (Supplementary Information, SI) according to
120 the similarity theory after the measurement of the wind speed and temperature profile (Yu and Sun, 2006).

121 **2.4 Quality control**

122 In order to ensure the accuracy of the measurement results, regularly maintenance and calibration was performed to the
123 continuous monitoring system at both two sites. The particulate filter membrane on the air intake was changed once a week.
124 In addition, the soda-lime tank after the air intake and the filter membrane before the Hg analyzer was replaced monthly. The
125 automatic calibrations of the internal mercury source of Tekran 2537X and Tekran 2537B ~~and manual calibration by mercury~~

126 ~~injection method~~ were done once every 24 h ~~and one month respectively~~. The manual calibration by placing the air intakes in
127 certain Hg concentration (Tekran 2505, Tekran Inc.) for 24h were done once every one month. The recovery rates were
128 between 95 to 105% with an average value of 100.3%.

129 We did blank experiments, i.e., measuring the detection limit of the concentration gradient for the monitoring systems before
130 the installation, when the air intakes were both placed indoor with stable mercury concentration. It turned out that the
131 differences of GEM concentration between the pipelines were $0.004 \pm 0.017 \text{ ng m}^{-3}$ and $0.010 \pm 0.024 \text{ ng m}^{-3}$ ($n > 60$) at QYZ
132 and HT sites, respectively. The detection limit of the concentration gradient of the system was defined as the mean of detecting
133 difference results plus one standard deviation (Fritsche et al., 2008b). Therefore, the detection limits were $0.021 \text{ ng}\cdot\text{m}^{-3}$ and
134 $0.034 \text{ ng}\cdot\text{m}^{-3}$ at QYZ and HT sites, respectively. It means that there was no significant difference between the two GEM
135 concentrations at different height when the discrepancy was lower than the detection limits in the field experiments. In addition,
136 the parallelity of the two pipelines in the system was detected every month by moving the air intakes to the cabin and run
137 continuously for at least 24 h. The pipeline need clean by soaking 24 h with 15% nitric acid then cleaning with ultrapure water
138 and acetone in turn, finally drying with zero mercury gas (Zero Air Tank, Tekran Inc.), until the difference of GEM
139 concentration between the two pipelines was less than 0.02 ng m^{-3} . There was a spare pipeline system at each site to avoid
140 the pause of monitoring due to pipeline cleaning. The blank experiments to measure the monitoring system error were
141 conducted before the installation by placing the air intakes in the zero mercury gas (Zero Air Tank, Tekran Inc.) for 48h. There
142 were almost no adsorption/emission from the monitoring system (including of the long Teflon tube, the soda-lime tank and the
143 electromagnetic valves) with the measurement results less than the detection limit of the instrument (0.1 ng m^{-3}).

144 The result measured by AGM represent a mean value of regional GEM flux, i.e, footprints area of tower, which is related to
145 the measuring height and meteorological conditions (Fritsche et al., 2008b). Previous study estimated that the footprint of
146 intake at 40 m height on the flux tower was 100 - 400 m (Zhao et al., 2005). Therefore, the footprints of the intakes located at
147 different height may be similar due to the relatively uniform distribution of *pinus massoniana* or *cunninghamia lanceolata*
148 forest within 500 m around the flux towers in our research.

149 The concentrations gradient lower than the system detection limit could not be truncated in case of the overestimation of GEM
150 flux when calculating the average GEM flux in previous studies (Fritsche et al., 2008b; Converse et al., 2010). The proportion
151 of the data which had the GEM concentration gradient larger than the detection limit in this study was larger than 85%, which
152 was higher than that in the previous study on grassland (about 50%; Fritsche et al., 2008b). The reason of such high quality
153 data might be the larger height difference (10m at QYZ site and 8m at HT site, vs. 2m in the grassland study), higher GEM
154 concentration, and larger exchange surface of forest than grassland. In accordance with the inaccurate measurement by AGM
155 under the high atmospheric stability (Converse et al., 2010), especially in temperature inversion, the calculation of turbulent
156 transfer coefficient K could not converge, and the flux would be eliminated. In addition, the data would be eliminated when
157 the GEM flux exceed the range of the monthly mean ± 3 standard deviations, or during instrument failure and operation
158 instability.

159 3 Results and discussion

160 3.1 Hourly and daily variations in GEM concentrations and fluxes

161 QYZ and HT stations have both subtropical monsoon climate, with hot and rainy summers, and cold and dry winters (Table
162 S2). Atmospheric GEM concentrations (the average concentration at two heights) were lower during spring and summer, and
163 higher in winter and fall, with an annual average value of 3.64 ng m^{-3} ($1.89 \sim 6.26 \text{ ng m}^{-3}$, 5% ~ 95% confidence interval) at
164 QYZ site (Figure 3), which was far higher than the mercury concentrations in background region in the ~~northern~~ Northern
165 ~~hemisphere~~ Hemisphere ($1.5 \sim 2.0 \text{ ng} \cdot \text{m}^{-3}$, Steffen et al., 2005; Kock et al., 2005; 1.51 ng·m⁻³ in 2014, Sprovieri et al., 2016;)
166 and correspond to the observed results in southeast China ($2.7 \sim 5.4 \text{ ng} \cdot \text{m}^{-3}$, Wang et al., 2014a). Although there were no major
167 anthropogenic mercury emission sources near the QYZ station, the high concentration may be attributed to regional residential
168 coal combustion (Wu et al., 2016) and high background GEM concentration in China (Fu et al., 2015). The annual average
169 GEM concentration at HT station was 5.93 ng m^{-3} ($2.46 \sim 11.6 \text{ ng m}^{-3}$, 5% ~ 95% confidence interval), even higher than that
170 at QYZ station, ~~because HT station was affected by WS Mercury Mine.~~

171 The diurnal variation of fluxes indicated that the GEM flux increased gradually with the increase in air temperature and solar
172 radiation in the daytime in all four seasons. The peak fluxes were averaged to 30.9 , 29.3 , 50.9 and $29.6 \text{ ng m}^{-2} \text{ h}^{-1}$ (22.6 , 46.2 ,
173 46.2 and $44.7 \text{ ng m}^{-2} \text{ h}^{-1}$) in winter (December - February), spring (March - May), summer (June - August) and fall (September
174 - November) respectively at QYZ (HT) at around 1:00 pm. In contrast, the GEM fluxes were stable at around zero or even
175 negative at night, indicating a state of Hg balance at QYZ site and a strong sink at HT site. This pattern was similar to the Hg
176 emission characteristics of soil (Ma et al., 2016), vegetation (Luo et al., 2016), and terrestrial surfaces (Stamenkovic et al.,
177 2008). Modelling results of the diurnal variation of GEM fluxes over canopy for deciduous needle-leaf forest (Wang et al.,
178 2016) also showed the similar trend.

179 A clear GEM absorption (negative fluxes) not only occurred at night but also in the morning in spring at both sites (Figure 4b).
180 A small and a large depletion peaked at 9:00 am and 11:00 am at QYZ and HT sites, respectively in spring might result from
181 the vegetation uptake, which was found by direct monitoring of GEM emission from foliage (Luo et al., 2016; Converse et al.,
182 2010; Stamenkovic and Gustin, 2009). The daytime-GEM emission fluxes were significantly higher in summer and lower in
183 winter with the changes of air temperature and solar radiation. With longer daytime and higher temperature, there were fewer
184 hours per day in a state of GEM sink in summer (Figure 4c). The atmosphere-forest exchange of GEM became weaker in the
185 fall as the decline in temperature and the dormant of plant growth (Figure 4d). There were also seasonal differences on diurnal
186 variation of GEM emission from soil (Ma et al., 2016) and vegetation (Luo et al., 2016), with highest values occurring in
187 summer, followed by spring and fall, while the lowest value in winter.

188 The two stations had the similar temperature due to the same climate condition and latitude (Table 1 and S2). Relatively higher
189 value and later peak of solar radiation (except for summer) at HT site might result from the higher altitude and lower longitude,
190 which would delay the peaks of emission flux in winter, spring, and fall. Relatively larger standard variance of GEM flux at

191 HT site indicated the higher fluctuation, which might be ascribed to the fluctuating GEM concentration. HT station is close to
192 WS Mercury Mine, the GEM concentration is vulnerable to the meteorological factors like wind direction.

193 3.2 Monthly variations in GEM concentrations and fluxes

194 The monthly mean value of GEM concentration seemed quite even throughout the year at both QYZ and HT Sites, with three
195 peak values in January, June, and November (4.52, 4.32, and 4.25 ng m⁻³ at QYZ site; 6.73, 6.74, and 7.14 ng m⁻³ at HT site),
196 and two bottom values of 2.33 and 2.89 ng m⁻³ (in March and July) at QYZ site and 4.29 and 3.34 ng m⁻³ (in February and July)
197 at HT site. In generally, monthly variations of fluxes exhibited an opposite trend of the concentration, almost all the larger
198 fluxes emerged in the months with lower GEM concentration.

199 All the monthly mean GEM fluxes were positive at QYZ station (Figure 5), indicating that the forest was net atmospheric
200 GEM source in each month. The relatively low GEM flux (3.13 ng m⁻² h⁻¹) and lowest air temperature (7.15 °C) occurred in
201 December. The monthly mean GEM fluxes rapidly rose from December to March, coinciding with the increase in air
202 temperature and solar radiation, followed by a sudden fall to 1.56 ng m⁻² h⁻¹ in April, and a slight increase to 4.40 ng m⁻² h⁻¹ in
203 June. After that, the GEM flux rapidly increased to 11.5 ng m⁻² h⁻¹ in July and peaked at August (12.8 ng m⁻² h⁻¹), then gradually
204 reduced to 6.84 ng m⁻² h⁻¹ in November, corresponding to the decrease in air temperature. Generally, the increase of solar
205 radiation and air temperature would cause the increasing in GEM emission from soil and vegetation (see section 3.3). The
206 monthly variations of annual Hg emission fluxes from forest soil in South Korea showed similar trend with air temperature
207 (Han et al., 2016). Mainly affected by soil emissions, the changes of GEM fluxes showed similar trend as those of air
208 temperature and solar radiation in winter and fall. In contrast, the GEM fluxes greatly decreased in the growing season, mainly
209 influenced by vegetation uptake of GEM (Millhollen et al., 2006a; Stamenkovic and Gustin, 2009).

210 Different from QYZ station, the forest was a GEM sink in November, December and January with a negative value of monthly
211 mean GEM flux of -6.82, -7.64, and -3.60 ng m⁻² h⁻¹ respectively at HT station (Figure 5). The monthly mean GEM fluxes
212 gradually elevated and became positive in February to April, subsequently fell to negative in May. Then, coinciding with the
213 change of air temperature, the GEM fluxes increased again, peaked in August (6.86 ng m⁻² h⁻¹), and gradually decreased to
214 negative in November. Although monthly variation of GEM fluxes at HT site was similar to that at QYZ site, HT site had
215 overall lower GEM fluxes but higher atmospheric GEM concentration than QYZ station. The annual average atmospheric
216 mercury concentration at HT site was 62% higher than that at QYZ site (Table 1). Higher concentrations of atmospheric
217 mercury would inhibit the Hg release from soil and plants, and increase the GEM absorption of foliage (see also in section
218 3.2). In addition to the influence of high atmospheric GEM concentration, the current-year foliage of *cunninghamia lanceolata*
219 (dominant species at HT station, Table 1) have larger absorption than *pinus massoniana* at QYZ indicated by larger Hg content
220 in needles and litters (Figure S4S3; Luo et al., 2016).

221 The monthly mean daytime-GEM fluxes always had positive values, which were much larger than the values at night (with
222 small negative values in December, January, April and May, and near-zero in other months) at QYZ site (Figure 6). Thus, the
223 GEM flux over forest canopy was mainly attributed to the emission during the daytime at QYZ site. The monthly mean GEM

224 fluxes were also positive during the daytime but all negative at night at HT site. HT site had larger monthly mean emission
225 fluxes during the daytime and larger absorption fluxes at night (Figure 6). As a total effect, the monthly fluxes were lower than
226 those in QYZ (Figure 5).

227 3.3 Factors influencing GEM flux

228 In order to evaluate the influences of the environmental conditions and atmospheric GEM concentration on the GEM fluxes,
229 the correlation analysis between the flux and each factor had been calculated (Table 2). It showed that the GEM flux over
230 forest canopy was negatively correlated with atmospheric GEM concentration at both sites except in summer at QYZ station.
231 The inhibiting effect of atmospheric GEM concentration on GEM emission was not only reflected by the lower emission fluxes
232 at HT site comparing with those in QYZ site (Figure 5), but also by an instant decline in GEM flux after a sudden increase in
233 ambient GEM concentration. For instance, continuous measurement data during five typical days in each season (Figure 7)
234 showed an absorption peak on February 3 and May 5 at QYZ site and ~~February 20~~, May 14 and August ~~23-24~~ at HT site caused
235 by the increase in air GEM concentrations. According to the wind direction records, the sudden rise of GEM concentration to
236 22.94 ng·m⁻³ on May 14 ~~and 21.21 ng m⁻³ August 24~~ at HT site might be caused by the approach of a high-mercury-content
237 air mass from WS Mercury Mine leading by northwest wind. Elevated ambient GEM concentration has been found to suppress
238 GEM flux by reducing the GEM concentration gradient at the interfacial surfaces (Xin and Gustin, 2007). At locations where
239 ambient Hg concentration is high, absorption (or deposition) is predominately observed despite of influence of meteorological
240 factors (Wang et al., 2007; Niu et al., 2011). Although the increase in GEM concentration would inhibit mercury emissions of
241 foliage and soil, the emission fluxes had positive correlation with atmospheric GEM concentration in summer (Figure ~~S2S4~~)
242 because the large emission of GEM concentration in hot summer might result in an increase of air mercury concentration.
243 The GEM flux was positively correlated with solar radiation, air temperature, and wind speed at both QYZ and HT sites (Table
244 2). Solar radiation has been found to be highly positively correlated with soil and vegetation GEM flux (Carpi and Lindberg,
245 1997; Boudala et al., 2000; Zhang et al., 2001; Gustin et al., 2002; Poissant et al., 2004; Bahlmann et al., 2006), because it can
246 enhance Hg²⁺ reduction and therefore facilitate GEM evasion (Gustin et al., 2002). For instance, there was a high GEM
247 emission peak at noon in winter (Figure 7; from February 1 to 3 at QYZ site and February 19 to 20 at HT site) even with
248 extremely low temperature. In addition to solar radiation, air temperature had significant effect on GEM flux, especially in
249 summer. Continued GEM emissions occurred in the daytime without strong solar radiation, or in the evening under the high
250 temperature in the summer (Figure 7; August 18 to 19 at QYZ site). Recent studies also showed that the GEM emission flux
251 from soil would be mainly controlled by the air temperature (Moore and Carpi, 2005; Bahlmann et al., 2006). Compared with
252 that in summer, GEM emission peak had decreased (Figure 7; 53.0 and 60.8 ng·m⁻³ h⁻¹ on November 9 and 10 vs. 77.6 on
253 August 16 at QYZ site; 213, 206 and 103 ng·m⁻³ h⁻¹ on November 15, 16 and 18 vs. 322 and 276 ng·m⁻³ h⁻¹ on August 21 and
254 22 9 in HT site) on the sunny day in the fall due to the decrease in temperature. In addition, as wind speed increased, the air
255 turbulence on the surface of soil and foliage would speed up, and thus enhance the desorption of GEM on the interface
256 (Wallschlager et al., 2002; Gillis and Miller, 2000; Eckley et al., 2010; Lin et al., 2012), which may explain the positive

257 correlation between GEM flux and wind speed. Soil temperature mainly impacting on the emission of soil, and also showed
258 positive correlation with GEM fluxes except for in the winter with low soil temperature (Table 2). One possible explanation
259 of the exception was that the change of soil temperature had no significant influence on the microbial activity and the reaction
260 rate in soil if soil temperature was lower than a certain value (Corbett-Hains et al., 2012).

261 Air humidity generally was negatively correlated to the GEM flux over forest canopy (Table 2). Higher relative humidity may
262 decrease stomatal conductance and thus lower transpiration of needles, which would result in decreases in GEM emissions
263 (Luo et al., 2016). The correlation between GEM flux and soil moisture was not sure at QYZ station, e.g., positive in winter,
264 negative in spring and fall, but no significance in summer. It seems that the influence of soil moisture on soil mercury emissions
265 was uncertain, depends on the state soil water saturation (Figure S3S5). Previous studies supported that adding water to dry
266 soil promotes Hg reduction, because water molecules likely replace soil GEM binding sites and facilitates GEM emission.
267 However, Hg emission is suppressed in water saturated soil because the soil pore space filled with water hampers Hg mass
268 transfer (Gillis and Miller, 2000; Gustin and Stamenkovic, 2005; Pannu et al., 2014). For instance, intensive soil GEM emission
269 was synchronized to the rainfall at around 9:00 pm on August 16 and 8:00 pm on August 17 at QYZ site (Figure 7). In addition,
270 the continuous but weaker rainfall from November 6 to 7 might also increase the GEM emission, in comparison with that in
271 November 8 under the same solar radiation and temperature. Actually, continuous but weaker rainfall would lead to the
272 increase of soil moisture, but not necessarily caused soil water saturation. Soil moisture content monitoring results had shown
273 that the soil moisture content had a certain rise but remained below 0.28 during this period, which was lower than the highest
274 value (0.52) during the annual monitoring. However, no significant emission flux was observed on August 19 after a series of
275 strong rainfall. Repeated rewetting experiments showed a smaller increase in emission, implying GEM needs to be resupplied
276 by means of reduction and dry deposition after a wetting event (Gustin and Stamenkovic, 2005; Song and Van Heyst, 2005;
277 Eckley et al., 2011). The correlation between GEM flux and soil moisture was not significant in all of the seasons since the
278 fluctuation of soil moisture content was small with the annual range of 0.21~0.34 at HT site, and the change of soil moisture
279 content had far less impact on the soil GEM emissions.

280 The temporal variation of vegetation growth would play an important role in the forest GEM emission because of the vital
281 function of vegetation to Hg cycle in forest ecosystem through changing environmental variables at ground surfaces (e.g.,
282 reducing solar radiation, temperature and friction velocity) (Gustin et al., 2004), and providing active surfaces for Hg uptake.
283 Recent measurements suggested that air–surface exchange of GEM is largely bidirectional between air and plant, and that
284 growing plants act as a net sink (Ericksen et al., 2003; Stamenkovic et al., 2008; Hartman et al., 2009). The negative exchange
285 GEM fluxes at night at both two sites in this study should be mainly attributed to GEM adsorption by vegetation (Figure 6).
286 In addition, GEM absorption capacity of foliage began to weaken at the end of growing season in November when the
287 absorption peaks were smaller than that in spring at both QYZ and HT sites (Figure 7). The stomata open in the morning will
288 also accelerate the forest absorption of Hg by vegetation, lead to the emergence of absorption peak even in the morning (Luo
289 et al., 2016).

290 3.4 Forest as source/sink of GEM

291 GEM flux measurements over forest canopy indicated that QYZ forest at the clean-mildly polluted site was a net source of
292 GEM in all seasons, with the highest and lowest GEM emissions in summer ($8.09 \text{ ng m}^{-2} \text{ h}^{-1}$) and spring ($5.25 \text{ ng m}^{-2} \text{ h}^{-1}$, early
293 growing season) respectively. In contrast, significant differences in GEM fluxes were observed among seasons at HT, the
294 contaminated-moderately polluted site, indicating a clear sink in winter (dormant season), a slight source in spring and fall,
295 and a large source in summer (Table 3). As the total effect, the forest ecosystem at HT site had a net GEM emission with a
296 magnitude of $1.210.30 \text{ ng m}^{-2} \text{ h}^{-1}$ for a whole year. These results suggest that the subtropical forests in our study region should
297 be the substantial GEM source, and the differences among seasons emphasized the importance of capturing GEM flux
298 seasonality when determining total Hg budgets. As mentioned before, there was almost no difference of climate conditions
299 between QYZ and HT sites, with the similar soil type and latitude, and little difference in the vegetation growth. However, the
300 HT site with higher atmospheric GEM concentration had relatively lower GEM fluxes in all seasons in comparison with those
301 in QYZ site. It emphasized again the importance of atmospheric GEM concentration on the GEM fluxes.

302 The GEM fluxes over forest canopy were the sum of emission fluxes from soil and vegetation, and extremely difficult to
303 quantify. GEM exchange of foliage/atmosphere or soil/atmosphere is both bi-directional, with net adsorption occurring at
304 elevated air Hg concentration while net emission when typical ambient concentration was lower than the “compensation point”
305 (Converse et al., 2010; Ericksen et al., 2003; Stamenkovic et al., 2008; Hartman et al., 2009). However, the study of
306 foliage/atmosphere mercury exchange at QYZ indicated that the vegetation presented as a net GEM source in all seasons as the
307 total effects with a value of $1.32 \text{ ng m}^{-2} \text{ h}^{-1}$ ($2.19, 0.32, 2.51$ and $-0.01 \text{ ng m}^{-2} \text{ h}^{-1}$ in winter, spring, summer and fall respectively)
308 caused by high rates of photoreduction and plant transpiration due to high temperature and radiation, relatively large leaf
309 surface area and elevated mercury deposition, but a clear sink in the growing season with stomatal opening (Luo et al., 2016)
310 even under the relatively lower atmospheric GEM concentration. In addition, the study of the mercury exchange between
311 atmosphere and soil under the forest canopy at QYZ using the DFC methods also showed the soil manifested as net GEM
312 sources at all the seasons (Figure S6. $0.13 \pm 0.43, 1.54 \pm 1.78, 4.76 \pm 1.86$ and $2.07 \pm 1.73 \text{ ng m}^{-2} \text{ h}^{-1}$ in winter, spring, summer
313 and fall, respectively; unpublished data). Thus, the net emissions observed at QYZ were contributed by both soil and foliar
314 emissions. The GEM fluxes over forest canopy ($8.09 \text{ ng m}^{-2} \text{ h}^{-1}$) in this study were almost similar to the sum ($7.27 \text{ ng m}^{-2} \text{ h}^{-1}$)
315 of emission fluxes from foliage and soil in summer, but had larger values in other seasons. It might be because of the
316 underestimation of the GEM fluxes from soil due to the decreased turbulence in chamber using the DFC method, and the lack
317 of GEM fluxes from the undergrowth vegetation. Although the foliage/atmosphere and soil/atmosphere mercury exchange at
318 HT have not been measured, respectively, the comparison of Hg content of current-year foliage and soil between two sites
319 might indicate that there were larger GEM emission fluxes from soil but much larger GEM adsorption by foliage. Until now,
320 there are merely few researches using AGM to monitor the GEM flux above forest canopy even in short period. Previous
321 studies showed that the exchange fluxes of GEM vary in sign and magnitude (Table 3). Lindberg et al. (1998) measured GEM
322 fluxes over a mature deciduous forest, a yang pine plantation, and a boreal forest floor using the MBR method and suggested

323 that global forest is a net source of GEM with an emission of 10-330, 17-86 and 1-4 ng m⁻² h⁻¹ at daytime, respectively (Table
324 3). The observation of Hg fluxes in a deciduous forest using a REA method showed a net GEM emission of 21.9 ng m⁻² h⁻¹
325 during summer (Bash and Miller, 2008). However, a study in Québec, Canada showed that GEM concentrations at a maple
326 forest site are consistently lower than those measured at an adjacent open site, indicating a Hg sink for the forest (Poissant et
327 al., 2008). Similarly, the lower GEM concentrations observed in leaf-growing season at forest sites across the Atmospheric
328 Mercury Network (AMNet) in USA (Lan et al., 2012), Coventry Connecticut, England (Bash and Miller, 2009), Mt. Changbai,
329 Northeast China (Fu et al., 2016) also suggest forest as a net GEM sink during the growing season. Different results were
330 obtained by AGM and MBR method at the same time (Converse et al., 2010) (Table 3). There was limiting comparability of
331 fluxes data reported in literature because of the lack of a standard method protocol for GEM flux quantification (Gustin, 2011;
332 Zhu et al., 2015). ~~Although t~~The discrepancy in the measured GEM exchanges between forest and atmosphere is partially
333 attributed to the uncertainties of the flux quantification method (Sommar et al., 2013), ~~but the~~ forest structure, climate condition,
334 background Hg concentration, and forest soil Hg content could play critical roles in GEM emission from forest ecosystem.
335 Unlike deciduous forest as a sink of GEM in most previous studies, the evergreen foliage with relatively higher LAI at all
336 seasons in the subtropical forests in this study (in spite of the seasonal variations of vegetation growth) was demonstrated as a
337 net GEM source to the atmosphere (Luo et al., 2016). Evergreen tree species generally have higher exchange capabilities of
338 GEM relative to deciduous tree species and result in high rates of photoreduction and plant transpiration under the high
339 temperature, solar radiation and soil Hg content. -In addition, extremely high soil Hg content (42.6 and 167 ng g⁻¹ at QYZ and
340 HT sites shown in Table 1, while 63 ng g⁻¹ in Québec, Canada; Poissant et al., 2008) result from long-term elevated Hg
341 deposition, the high temperature and solar radiation would also contribute the net emission flux of GEM from ~~both~~-forest soil
342 ~~and vegetation~~ in subtropical, south China. However, the observations in this study were not higher than the results in the
343 forests as GEM sources in previous studies, possibly due to the higher ambient GEM concentration (3.64 and 5.93 ng m⁻³ at
344 QYZ and HT sites vs. 2.23 ng m⁻³ in Tennessee, USA and 1.34 in Connecticut, USA; Table 3). Although there were net GEM
345 emissions (58.5 µg m⁻² yr⁻¹) from forest in this study at QYZ site based on the measurement of the GEM fluxes over forest
346 canopy, on account of extremely large Hg deposition (wet deposition: 14.4 µg m⁻² yr⁻¹; dry deposition: 52.5 µg m⁻² yr⁻¹; Luo et
347 al., 2016), the forest presented as a Hg source, overall.

348 4 Conclusions and implication

349 The high quality direct observation data of a ~~clean-mildly polluted~~ and a ~~contaminated-moderately polluted~~ site with typical
350 climate, vegetation type and soil type in south China could be important for implications for the regional Hg cycling estimation,
351 and the awareness of the role of forests in the global mercury cycle. From continuously quantitative MM-flux measurements
352 covering wide temporal scales at QYZ and HT sites in subtropical south China, it is inferred that forest ecosystems can
353 represent a net GEM source with the average magnitudes of 6.67 and 1.21 ng m⁻² h⁻¹ for a full year at a ~~clean-mildly polluted~~
354 site (QYZ) and a ~~contaminated-moderately polluted~~ site (HT), respectively. GEM flux measurements were net source in all

355 seasons at the clean-mildly polluted site, with the highest in summer because of the relatively high air temperature and radiation,
356 and lowest in spring result from the vegetation growth. For the contaminated-moderately polluted site, a net sink occurred in
357 the winter, a significant source in summer, and no significant flux during spring and fall. The GEM emission dominated in the
358 daytime, and peaked at around 1:00 pm, while the forest served as a GEM sink or balance at night. It is worth noting that there
359 was a lower emission fluxes of GEM at the contaminated-moderately polluted site result from similar or even higher emission
360 fluxes during daytime, but much higher adsorption fluxes at night than the clean-mildly polluted site –under the similar
361 meteorological conditions. Although, the larger Hg content in soil would enhance the emission of soil and vegetation, the
362 elevated GEM concentration suppresses the Hg emission, and increase the absorption by vegetation at the contaminated
363 moderately polluted site. The result indicated that the atmospheric GEM concentration play an importance role in inhibiting
364 the GEM fluxes between forest and air, coinciding with the negative correlation between GEM fluxes and atmospheric GEM
365 concentration. In addition, the forest should be pay attention as a critical increasing source with the decline atmospheric GEM
366 concentration because the Hg emission abatement in the future, and the increasing emission might result from the re-emission
367 of legacy Hg stored in the forest.

368 The GEM flux over forest canopy was the sum emission flux of soil and vegetation, and showed monthly variations caused by
369 the temporal variation of vegetation growth, atmospheric GEM concentration and meteorological conditions including of air
370 temperature, radiation and wind speed. The correlation between GEM fluxes and factors had been analysed, combined with
371 the characteristics of GEM exchange between soil (or foliage) and air. It indicated that GEM fluxes were positively correlated
372 with air temperature, soil temperature, wind speed, and solar radiation, but negatively correlated with air humidity. The
373 influence of soil moisture content was uncertain, depends on whether the soil water saturated and the initial state of the soil.
374 In addition, vegetation growth would play an important role in the decline in forest GEM emission in spring. The difference
375 in climate conditions and ambient GEM concentration should be considered when estimating the global forest GEM emission.

376 **Acknowledgement**

377 The authors are grateful for the financial support of the National Basic Research Program of China (No. 2013CB430000) and
378 the National Natural Science Foundation of China (No. 21377064 and No. 21221004). The authors also greatly acknowledge
379 the supports from Qianyanzhou Forest Experimental Station and Huitong Forest Experimental Station, and the help in system
380 maintenance from Yuanfen Huang and Yungui Yang.

381 **References**

382 Bahlmann, E., Ebinghaus, R., and Ruck, W.: Development and application of a laboratory flux measurement system (LFMS)
383 for the investigation of the kinetics of mercury emissions from soils, *Journal of Environmental Management*, 81, 114-
384 125, 10.1016/j.jenvman.2005.09.022, 2006.

385 Bash, J. O., and Miller, D. R.: A relaxed eddy accumulation system for measuring surface fluxes of total gaseous mercury,
386 *Journal of Atmospheric and Oceanic Technology*, 25, 244-257, 10.1175/2007jtecha908.1, 2008.

387 Bash, J. O., and Miller, D. R.: Growing season total gaseous mercury (TGM) flux measurements over an *Acer rubrum* L. stand,
388 *Atmos. Environ.*, 43, 5953-5961, 10.1016/j.atmosenv.2009.08.008, 2009.

389 Baya, A. P., and Van Heyst, B.: Assessing the trends and effects of environmental parameters on the behaviour of mercury in
390 the lower atmosphere over cropped land over four seasons, *Atmos. Chem. Phys.*, 10, 8617-8628, 10.5194/acp-10-8617-
391 2010, 2010.

392 Boudala, F. S., Folkins, I., Beauchamp, S., Tordon, R., Neima, J., and Johnson, B.: Mercury flux measurements over air and
393 water in Kejimikujik National Park, Nova Scotia, *Water Air Soil Pollut.*, 122, 183-202, 10.1023/a:1005299411107, 2000.

394 Carpi, A., and Lindberg, S. E.: Sunlight-mediated emission of elemental mercury from soil amended with municipal sewage
395 sludge, *Environ. Sci. Technol.*, 31, 2085-2091, 10.1021/es960910+, 1997.

396 CAS., C., (The China Vegetation Editorial Committee, Chinese Academy of Science): *Vegetation map of the People's*
397 *Republic of China (1:1000 000)*, 2007. (In Chinese)

398 Cobbett, F. D., Steffen, A., Lawson, G., and Van Heyst, B. J.: GEM fluxes and atmospheric mercury concentrations (GEM,
399 RGM and Hg-P) in the Canadian Arctic at Alert, Nunavut, Canada (February-June 2005), *Atmos. Environ.*, 41, 6527-
400 6543, 10.1016/j.atmosenv.2007.04.033, 2007.

401 Cobbett, F. D., and Van Heyst, B. J.: Measurements of GEM fluxes and atmospheric mercury concentrations (GEM, RGM
402 and Hg-P) from an agricultural field amended with biosolids in Southern Ont., Canada (October 2004-November 2004),
403 *Atmos. Environ.*, 41, 2270-2282, 10.1016/j.atmosenv.2006.11.011, 2007.

404 Converse, A. D., Riscassi, A. L., and Scanlon, T. M.: Seasonal variability in gaseous mercury fluxes measured in a high-
405 elevation meadow, *Atmos. Environ.*, 44, 2176-2185, 10.1016/j.atmosenv.2010.03.024, 2010.

406 Corbett-Hains, H., Walters, N. E., and Van Heyst, B. J.: Evaluating the effects of sub-zero temperature cycling on mercury
407 flux from soils, *Atmos. Environ.*, 63, 102-108, 10.1016/j.atmosenv.2012.09.047, 2012.

408 Driscoll, C. T., Mason, R. P., Chan, H. M., Jacob, D., and Pirrone, N.: Mercury as a global pollutant: sources, pathways and
409 effects, *Environ. Sci. Technol.*, 47, 4967-4983, 2013.

410 Eckley, C. S., Gustin, M., Lin, C. J., Li, X., and Miller, M. B.: The influence of dynamic chamber design and operating
411 parameters on calculated surface-to-air mercury fluxes, *Atmos. Environ.*, 44, 194-203, 10.1016/j.atmosenv.2009.10.013,
412 2010.

413 Eckley, C. S., Gustin, M., Miller, M. B., and Marsik, F.: Scaling non-point-source mercury emissions from two active industrial
414 gold mines: influential variables and annual emission estimates, *Environ. Sci. Technol.*, 45, 392-399, 10.1021/es101820q,
415 2011.

416 Engle, M. A., Gustin, M. S., Lindberg, S. E., Gertler, A. W., and Ariya, P. A.: The influence of ozone on atmospheric emissions
417 of gaseous elemental mercury and reactive gaseous mercury from substrates, *Atmos. Environ.*, 39, 7506-7517,
418 10.1016/j.atmosenv.2005.07.069, 2005.

419 Ericksen, J. A., Gustin, M. S., Schorran, D. E., Johnson, D. W., Lindberg, S. E., and Coleman, J. S.: Accumulation of
420 atmospheric mercury in forest foliage, *Atmos. Environ.*, 37, 1613-1622, 10.1016/s1352-2310(03)00008-6, 2003.

421 Frescholtz, T. F., Gustin, M. S., Schorran, D. E., and Fernandez, G. C. J.: Assessing the source of mercury in foliar tissue of
422 quaking aspen, *Environmental Toxicology and Chemistry*, 22, 2114-2119, 10.1897/1551-
423 5028(2003)022<2114:atsomi>2.0.co;2, 2003.

424 Fritsche, J., Obrist, D., and Alewell, C.: Evidence of microbial control of Hg⁰ emissions from uncontaminated terrestrial soils,
425 *Journal of Plant Nutrition and Soil Science-Zeitschrift Fur Pflanzenernahrung Und Bodenkunde*, 171, 200-209,
426 10.1002/jpln.200625211, 2008a.

427 Fritsche, J., Obrist, D., Zeeman, M. J., Conen, F., Eugster, W., and Alewell, C.: Elemental mercury fluxes over a sub-alpine
428 grassland determined with two micrometeorological methods, *Atmos. Environ.*, 42, 2922-2933,
429 10.1016/j.atmosenv.2007.12.055, 2008b.

430 Fritsche, J., Wohlfahrt, G., Ammann, C., Zeeman, M., Hammerle, A., Obrist, D., and Alewell, C.: Summertime elemental
431 mercury exchange of temperate grasslands on an ecosystem-scale, *Atmos. Chem. Phys.*, 8, 7709-7722, 2008c.

432 [Fu, X. W., Zhang, H., Wang, X., Yu, B., Lin, C. J., and Feng, X. B.: Observations of atmospheric mercury in China: a critical](#)
433 [review. *Atmospheric Chemistry & Physics Discussions*, 15, 11925-11983, 2015.](#)

434

435 Fu, X., Zhu, W., Zhang, H., Sommar, J., Yu, B., Yang, X., Wang, X., Lin, C.-J., and Feng, X.: Depletion of atmospheric
436 gaseous elemental mercury by plant uptake at Mt. Changbai, Northeast China, *Atmos. Chem. Phys.*, 16, 12861-12873,
437 10.5194/acp-16-12861-2016, 2016.

438 Gao, Y., He, N., Yu, G., Chen, W., and Wang, Q.: Long-term effects of different land use types on C, N, and P stoichiometry
439 and storage in subtropical ecosystems: A case study in China, *Ecological Engineering*, 67, 171-181, 2014.

440 Gillis, A. A., and Miller, D. R.: Some local environmental effects on mercury emission and absorption at a soil surface, *Sci.*
441 *Total Environ.*, 260, 191-200, 10.1016/s0048-9697(00)00563-5, 2000.

442 Grigal, D. F.: Mercury sequestration in forests and peatlands: A review, *Journal of Environmental Quality*, 32, 393-405, 2003.

443 Gustin, M., and Jaffe, D.: Reducing the uncertainty in measurement and understanding of mercury in the atmosphere, *Environ.*
444 *Sci. Technol.*, 44, 2222-2227, 10.1021/es902736k, 2010.

445 Gustin, M. S., Biester, H., and Kim, C. S.: Investigation of the light-enhanced emission of mercury from naturally enriched
446 substrates, *Atmos. Environ.*, 36, 3241-3254, 10.1016/s1352-2310(02)00329-1, 2002.

447 Gustin, M. S., Ericksen, J. A., Schorran, D. E., Johnson, D. W., Lindberg, S. E., and Coleman, J. S.: Application of controlled
448 mesocosms for understanding mercury air-soil-plant exchange, *Environ. Sci. Technol.*, 38, 6044-6050,
449 10.1021/es0487933, 2004.

450 Gustin, M. S., and Stamenkovic, J.: Effect of watering and soil moisture on mercury emissions from soils, *Biogeochemistry*,
451 76, 215-232, 10.1007/s10533-005-4566-8, 2005.

452 Gustin, M. S.: Exchange of mercury between the atmosphere and terrestrial ecosystems, 423-451 pp., 2011.

453 Han, J.-S., Seo, Y.-S., Kim, M.-K., Holsen, T. M., and Yi, S.-M.: Total atmospheric mercury deposition in forested areas in
454 South Korea, *Atmos. Chem. Phys.*, 16, 7653-7662, 10.5194/acp-16-7653-2016, 2016.

455 Hartman, J. S., Weisberg, P. J., Pillai, R., Ericksen, J. A., Kuiken, T., Lindberg, S. E., Zhang, H., Rytuba, J. J., and Gustin, M.
456 S.: Application of a Rule-Based Model to estimate mercury exchange for three background biomes in the Continental
457 United States, *Environ. Sci. Technol.*, 43, 4989-4994, 10.1021/es900075q, 2009.

458 Holmes, C. D., Jacob, D. J., Corbitt, E. S., Mao, J., Yang, X., Talbot, R., and Slemr, F.: Global atmospheric model for mercury
459 including oxidation by bromine atoms, *Atmos. Chem. Phys.*, 10, 12037-12057, 10.5194/acp-10-12037-2010, 2010.

460 Kim, K. H., Kim, M. Y., and Lee, G.: The soil-air exchange characteristics of total gaseous mercury from a large-scale
461 municipal landfill area, *Atmos. Environ.*, 35, 3475-3493, 10.1016/s1352-2310(01)00095-4, 2001.

462 Kim, K. H., Kim, M. Y., Kim, J., and Lee, G.: Effects of changes in environmental conditions on atmospheric mercury
463 exchange: Comparative analysis from a rice paddy field during the two spring periods of 2001 and 2002, *Journal of*
464 *Geophysical Research-Atmospheres*, 108, 10.1029/2003jd003375, 2003.

465 Kock, H. H., Bieber, E., Ebinghaus, R., Spain, T. G., and Thees, B.: Comparison of long-term trends and seasonal variations
466 of atmospheric mercury concentrations at the two European coastal monitoring stations Mace Head, Ireland, and Zingst,
467 Germany, *Atmos. Environ.*, 39, 7549-7556, 10.1016/j.atmosenv.2005.02.059, 2005.

468 Lan, X., Talbot, R., Castro, M., Perry, K., and Luke, W.: Seasonal and diurnal variations of atmospheric mercury across the
469 US determined from AMNet monitoring data, *Atmos. Chem. Phys.*, 12, 10569-10582, 10.5194/acp-12-10569-2012, 2012.

470 Lee, X., Benoit, G., and Hu, X. Z.: Total gaseous mercury concentration and flux over a coastal saltmarsh vegetation in
471 Connecticut, USA, *Atmos. Environ.*, 34, 4205-4213, 10.1016/s1352-2310(99)00487-2, 2000.

472 Lin, C.-J., Zhu, W., Li, X., Feng, X., Sommar, J., and Shang, L.: Novel dynamic flux chamber for measuring air-surface
473 exchange of Hg⁰ from soils, *Environ. Sci. Technol.*, 46, 8910-8920, 10.1021/es3012386, 2012.

474 Lindberg, S., Bullock, R., Ebinghaus, R., Engstrom, D., Feng, X., Fitzgerald, W., Pirrone, N., Prestbo, E., and Seigneur, C.: A
475 synthesis of progress and uncertainties in attributing the sources of mercury in deposition, *Ambio*, 36, 19-32, 2007.

476 Lindberg, S. E., Hanson, P. J., Meyers, T. P., and Kim, K. H.: Air/surface exchange of mercury vapor over forests - The need
477 for a reassessment of continental biogenic emissions, *Atmos. Environ.*, 32, 895-908, 10.1016/s1352-2310(97)00173-8,
478 1998.

479 Lindqvist, Johansson, Aastrup, Andersson, Bringmark, Hovsenius, Håkanson, Iverfeldt, Meili, and Timm: Mercury in the
480 Swedish environment, *Water Air & Soil Pollution*, 55, 1-261, 1991.

481 Luo, Y., Duan, L., Driscoll, C. T., Xu, G., Shao, M., Taylor, M., Wang, S., and Hao, J.: Foliage/atmosphere exchange of
482 mercury in a subtropical coniferous forest in south China, *J. Geophys. Res.-Biogeosci.*, 121, 2006-2016,
483 10.1002/2016jg003388, 2016.

484 Ma, M., Wang, D., Du, H., Sun, T., Zhao, Z., Wang, Y., and Wei, S.: Mercury dynamics and mass balance in a subtropical
485 forest, southwestern China, *Atmos. Chem. Phys.*, 16, 4529-4537, 10.5194/acp-16-4529-2016, 2016.

486 Mauclair, C., Layshock, J., and Carpi, A.: Quantifying the effect of humic matter on the emission of mercury from artificial
487 soil surfaces, *Appl. Geochem.*, 23, 594-601, 10.1016/j.apgeochem.2007.12.017, 2008.

488 Millhollen, A. G., Gustin, M. S., and Obrist, D.: Foliar mercury accumulation and exchange for three tree species, *Environ.*
489 *Sci. Technol.*, 40, 6001-6006, 10.1021/es0609194, 2006a.

490 Millhollen, A. G., Obrist, D., and Gustin, M. S.: Mercury accumulation in grass and forb species as a function of atmospheric
491 carbon dioxide concentrations and mercury exposures in air and soil, *Chemosphere*, 65, 889-897,
492 10.1016/j.chemosphere.2006.03.008, 2006b.

493 Moore, C., and Carpi, A.: Mechanisms of the emission of mercury from soil: role of UV radiation, *Journal of Geophysical*
494 *Research-Part D-Atmospheres*, 110, 9 pp.-9 pp., 10.1029/2004jd005567, 2005.

495 Niu, Z., Zhang, X., Wang, Z., and Ci, Z.: Field controlled experiments of mercury accumulation in crops from air and soil,
496 *Environ. Pollut.*, 159, 2684-2689, 10.1016/j.envpol.2011.05.029, 2011.

497 Obrist, D.: Atmospheric mercury pollution due to losses of terrestrial carbon pools?, *Biogeochemistry*, 85, 119-123,
498 10.1007/s10533-007-9108-0, 2007.

499 Pannu, R., Siciliano, S. D., and O'Driscoll, N. J.: Quantifying the effects of soil temperature, moisture and sterilization on
500 elemental mercury formation in boreal soils, *Environ. Pollut.*, 193, 138-146, 10.1016/j.envpol.2014.06.023, 2014.

501 Pirrone, N., Cinnirella, S., Feng, X., Finkelman, R. B., Friedli, H. R., Leaner, J., Mason, R., Mukherjee, A. B., Stracher, G. B.,
502 Streets, D. G., and Telmer, K.: Global mercury emissions to the atmosphere from anthropogenic and natural sources,
503 *Atmos. Chem. Phys.*, 10, 5951-5964, 10.5194/acp-10-5951-2010, 2010.

504 Poissant, L., Pilote, M., Constant, P., Beauvais, C., Zhang, H. H., and Xu, X. H.: Mercury gas exchanges over selected bare
505 soil and flooded sites in the bay St. Francois wetlands (Quebec, Canada), *Atmos. Environ.*, 38, 4205-4214,
506 10.1016/j.atmosenv.2004.03.068, 2004.

507 Poissant, L., Pilote, M., Yumvihoze, E., and Lean, D.: Mercury concentrations and foliage/atmosphere fluxes in a maple forest
508 ecosystem in Quebec, Canada, *Journal of Geophysical Research-Atmospheres*, 113, 10.1029/2007jd009510, 2008.

509 Rinklebe, J., Doring, A., Overesch, M., Du Laing, G., Wennrich, R., Staerk, H.-J., and Mothes, S.: Dynamics of mercury fluxes
510 and their controlling factors in large Hg-polluted floodplain areas, *Environ. Pollut.*, 158, 308-318,
511 10.1016/j.envpol.2009.07.001, 2010.

512 Schroeder, W. H., Anlauf, K. G., Barrie, L. A., Lu, J. Y., Steffen, A., Schneeberger, D. R., and Berg, T.: Arctic springtime
513 depletion of mercury, *Nature*, 394, 331-332, 10.1038/28530, 1998.

514 Sigler, J. M., Mao, H., and Talbot, R.: Gaseous elemental and reactive mercury in Southern New Hampshire, *Atmos. Chem.*
515 *Phys.*, 9, 1929-1942, 2009.

516 Sommar, J., Zhu, W., Lin, C.-J., and Feng, X.: Field Approaches to measure Hg exchange between natural surfaces and the
517 atmosphere a review, *Critical Reviews in Environmental Science and Technology*, 43, 1657-1739,
518 10.1080/10643389.2012.671733, 2013.

519 Song, S., Selin, N. E., Soerensen, A. L., Angot, H., Artz, R., Brooks, S., Brunke, E. G., Conley, G., Dommergue, A., Ebinghaus,
520 R., Holsen, T. M., Jaffe, D. A., Kang, S., Kelley, P., Luke, W. T., Magand, O., Marumoto, K., Pfaffhuber, K. A., Ren, X.,
521 Sheu, G. R., Slemr, F., Warneke, T., Weigelt, A., Weiss-Penzias, P., Wip, D. C., and Zhang, Q.: Top-down constraints
522 on atmospheric mercury emissions and implications for global biogeochemical cycling, *Atmos. Chem. Phys.*, 15, 7103-
523 7125, 10.5194/acp-15-7103-2015, 2015.

524 Song, X. X., and Van Heyst, B.: Volatilization of mercury from soils in response to simulated precipitation, *Atmos. Environ.*,
525 39, 7494-7505, 10.1016/j.atmosenv.2005.07.064, 2005.

526 Sprovieri, F., Pirrone, N., Bencardino, M., D'Amore, F., Carbone, F., Cinnirella, S., Mannarino, V., Landis, M., Ebinghaus,
527 R., and Weigelt, A.: Atmospheric mercury concentrations observed at ground-based monitoring sites globally distributed
528 in the framework of the GMOS network, *Atmospheric Chemistry & Physics*, 16, 1-32, 2016.

529

530 St Louis, V. L., Rudd, J. W. M., Kelly, C. A., Hall, B. D., Rolfhus, K. R., Scott, K. J., Lindberg, S. E., and Dong, W.:
531 Importance of the forest canopy to fluxes of methyl mercury and total mercury to boreal ecosystems, *Environ. Sci.*
532 *Technol.*, 35, 3089-3098, 10.1021/es001924p, 2001.

533 Stamenkovic, J., Gustin, M. S., Arnone, J. A., III, Johnson, D. W., Larsen, J. D., and Verburg, P. S. J.: Atmospheric mercury
534 exchange with a tallgrass prairie ecosystem housed in mesocosms, *Sci. Total Environ.*, 406, 227-238,
535 10.1016/j.scitotenv.2008.07.047, 2008.

536 Stamenkovic, J., and Gustin, M. S.: Nonstomatal versus stomatal uptake of atmospheric mercury, *Environ. Sci. Technol.*, 43,
537 1367-1372, 10.1021/es801583a, 2009.

538 Steffen, A., Schroeder, W., Macdonald, R., Poissant, L., and Konoplev, A.: Mercury in the Arctic atmosphere: An analysis of
539 eight years of measurements of GEM at Alert (Canada) and a comparison with observations at Amderma (Russia) and
540 Kuujjuarapik (Canada), *Sci. Total Environ.*, 342, 185-198, 10.1016/j.scitotenv.2004.12.048, 2005.

541 Streets, D. G., Zhang, Q., and Wu, Y.: Projections of Global Mercury Emissions in 2050, *Environ. Sci. Technol.*, 43, 2983-
542 2988, 10.1021/es802474j, 2009.

543 Streets, D. G., Devane, M. K., Lu, Z., Bond, T. C., Sunderland, E. M., and Jacob, D. J.: All-Time releases of mercury to the
544 atmosphere from human activities, *Environ. Sci. Technol.*, 45, 10485-10491, 10.1021/es202765m, 2011.

545 UNEP Minamata Convention on Mercury: available at: <http://www.mercuryconvention.org> (last access: 25 March 2017), 2013.

546 Wallschläger, D., Kock, H. H., Schroeder, W. H., Lindberg, S. E., Ebinghaus, R., and Wilken, R. D.: Estimating gaseous
547 mercury emissions from contaminated floodplain soils to the atmosphere with simple field measurement techniques,
548 *Water Air Soil Pollut.*, 135, 39-54, 10.1023/a:1014711831589, 2002.

549 Wang, L., Wang, S., Zhang, L., Wang, Y., Zhang, Y., Nielsen, C., McElroy, M. B., and Hao, J.: Source apportionment of
550 atmospheric mercury pollution in China using the GEOS-Chem model, *Environ. Pollut.*, 190, 166-175,
551 10.1016/j.envpol.2014.03.011, 2014a.

552 Wang, Q., Wang, S., and Zhang, J.: Assessing the effects of vegetation types on carbon storage fifteen years after reforestation
553 on a Chinese fir site, *For. Ecol. Manage.*, 258, 1437-1441, 10.1016/j.foreco.2009.06.050, 2009.

554 Wang, S., Feng, X., Qiu, G., Fu, X., and Wei, Z.: Characteristics of mercury exchange flux between soil and air in the heavily
555 air-polluted area, eastern Guizhou, China, *Atmos. Environ.*, 41, 5584-5594, 10.1016/j.atmosenv.2007.03.002, 2007.

556 Wang, X., Lin, C. J., and Feng, X.: Sensitivity analysis of an updated bidirectional air-surface exchange model for elemental
557 mercury vapor, *Atmos. Chem. Phys.*, 14, 6273-6287, 10.5194/acp-14-6273-2014, 2014b.

558 Wang, X., Lin, C.-J., Yuan, W., Sommar, J., Zhu, W., and Feng, X.: Emission-dominated gas exchange of elemental mercury
559 vapor over natural surfaces in China, *Atmos. Chem. Phys.*, 16, 11125-11143, 10.5194/acp-16-11125-2016, 2016.

560 Wu, Q., Wang, S., Li, G., Liang, S., Lin, C.-J., Wang, Y., Cai, S., Liu, K., and Hao, J.: Temporal Trend and Spatial Distribution
561 of Speciated Atmospheric Mercury Emissions in China During 1978-2014, *Environ. Sci. Technol.*, 50, 13428-13435,
562 10.1021/acs.est.6b04308, 2016.

563 Xin, M., and Gustin, M. S.: Gaseous elemental mercury exchange with low mercury containing soils: Investigation of
564 controlling factors, *Appl. Geochem.*, 22, 1451-1466, 10.1016/j.apgeochem.2007.02.006, 2007.

565 Yu, G., and Sun, X.: The principle and method of terrestrial ecosystems flux observations. Higher Education Press, Beijing,
566 2006. (In Chinese)

567 Zhang, H., Lindberg, S. E., Marsik, F. J., and Keeler, G. J.: Mercury air/surface exchange kinetics of background soils of the
568 Tahquamenon River watershed in the Michigan Upper Peninsula, *Water Air Soil Pollut.*, 126, 151-169,
569 10.1023/a:1005227802306, 2001.

570 Zhang, H., Lindberg, S. E., and Kuiken, T.: Mysterious diel cycles of mercury emission from soils held in the dark at constant
571 temperature, *Atmos. Environ.*, 42, 5424-5433, 10.1016/j.atmosenv.2008.02.037, 2008.

572 Zhang, L., Wang, S., Wang, L., Wu, Y., Duan, L., Wu, Q., Wang, F., Yang, M., Yang, H., Hao, J., and Liu, X.: Updated
573 emission inventories for speciated atmospheric mercury from anthropogenic sources in China, *Environ. Sci. Technol.*, 49,
574 3185-3194, 10.1021/es504840m, 2015.

575 Zhang, Y., Jacob, D. J., Horowitz, H. M., Chen, L., Amos, H. M., Krabbenhoft, D. P., Slemr, F., St Louis, V. L., and Sunderland,
576 E. M.: Observed decrease in atmospheric mercury explained by global decline in anthropogenic emissions, *Proceedings*
577 *of the National Academy of Sciences of the United States of America*, 113, 526-531, 10.1073/pnas.1516312113, 2016.

578 Zhao, X., Guan, D., Wu, J., Jin, C., Han, S.: Distribution of footprint and flux source area of the mixed forest of broad-leaved
579 and Korean pine in Changbai Mountain, *Journal of Beijing Forestry University*, 27, 17-22, 2005.

580 Zhu, W., Sommar, J., Lin, C. J., and Feng, X.: Mercury vapor air-surface exchange measured by collocated
581 micrometeorological and enclosure methods - Part I: Data comparability and method characteristics, *Atmos. Chem. Phys.*,
582 15, 685-702, 10.5194/acp-15-685-2015, 2015.

583 Zhu, W., Lin, C.-J., Wang, X., Sommar, J., Fu, X., and Feng, X.: Global observations and modeling of atmosphere-surface
584 exchange of elemental mercury: a critical review, *Atmos. Chem. Phys.*, 16, 4451-4480, 10.5194/acp-16-4451-2016, 2016.

585

Station sites	QYZ	HT
Location	115°04'E, 26°45'N	109°45'E, 26°50'N
Administrative region	Guanxi town, Jiangxi province	Guangping town, Hunan province
Altitude (m)	30~60	280~390
Climate type	Humid subtropical monsoon climate	
Mean annual temperature (°C) ^a	18.6	15.8
Mean annual precipitation (mm) ^a	1361	1200
<u>Dominated Vegetation-tree species (relative abundance) type</u>	<i>Pinus massoniana</i> (86.5%)	<i>Cunninghamia lanceolata</i> (92.4%)
<u>Other predominant vegetative species</u>	<i>Pinus elliottii</i> ; <i>Quercus fabei</i> ; <i>Vitex negundo</i> ; <i>Rhododendron plonch</i> ; <i>Ischaemum indicum</i>	<i>Marsa japonica</i> ; <i>Ilex pirlpurea</i> ; <i>Cyclosorus parasticus</i> ; <i>Woodwardia prolifera</i>
Forest age	31	27
Canopy height (m)	16	14
<u>Leaf area index (LAI) in summer</u>	<u>4.31</u>	<u>7.00</u>
<u>Canopy density</u>	<u>0.7</u>	<u>0.8</u>
<u>Radiation transfer under canopy</u>	<u>3.0%</u>	<u>2.7%</u>
Dominant soil type (Chinese soil name)	Udic Ferrisols (Red Earth)	Haplic Acrisol (Yellow Earth)
Organic matter content in surface soil (g kg ⁻¹) ^a	10~15	28.3
Soil pH ^a	4.52	3.85
Annual average GEM concentration (ng m ⁻³) ^b	3.64 ± 1.82	5.93 ± 3.16

Hg content in soil organic layer (ng g ⁻¹) ^c	76.2 ± 6.0	153 ± 28
Hg content in surface (0~5 cm) soil (ng g ⁻¹) ^c	42.6 ± 2.3	167 ± 32

587 ^a Data of QYZ and HT stations according to Gao et al. (2014) and Wang et al. (2009), respectively;

588 ^b Mean value of the measurements at the height of 25 m and 35 m at QYZ site, 22.5 and 30.5 m at HT site;

589 ^c Analyzed based on 18 samples using a direct Hg analyzer (DMA80, Milestone Inc., Italy).

590

591

593 **Table 2.** Pearson's correlation coefficient between GEM flux over forest canopy and atmospheric GEM concentration or each environmental
 594 factor.

Factors	Sites	Winter	Spring	Summer	Fall
GEM concentration	QYZ	-0.142**	-0.155**	0.014	-0.141**
	HT	-0.232**	-0.226**	-0.197**	-0.183**
Air temperature	QYZ	0.272**	0.166**	0.31**	0.298**
	HT	0.143**	0.121**	0.188**	0.135**
Air humidity	QYZ	-0.314**	-0.003	-0.293**	-0.339**
	HT	-0.101*	-0.149**	-0.246**	-0.255**
Wind speed	QYZ	0.159**	0.176**	0.162**	0.166**
	HT	0.119**	0.180**	0.106**	0.162**
Soil temperature	QYZ	0.025	0.165**	0.288**	0.175**
	HT	0.015	0.174**	0.253**	0.201**
soil moisture	QYZ	0.102**	-0.198**	0.03	-0.106**
	HT	0.001	-0.032	-0.003	0.034
Radiation	QYZ	0.628**	0.403**	0.401**	0.209**
	HT	0.265**	0.212**	0.313**	0.201**

595 * Significant at $p < 0.01$ level;

596 ** Significant at $p < 0.001$ level.

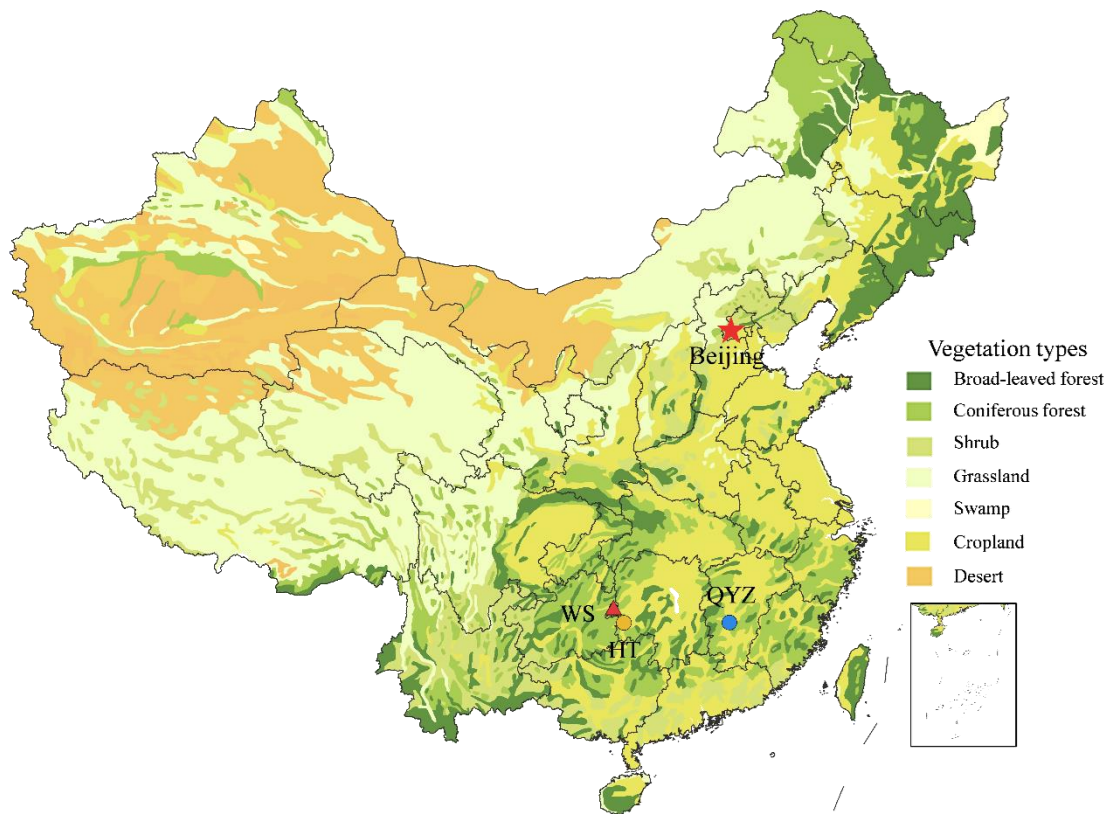
597

598 **Table 3.** Comparison of the GEM flux ($\text{ng}\cdot\text{m}^{-2}\cdot\text{h}^{-1}$) from different the observations.

Vegetation type	Location	winter	spring	summer	fall	GEM con	method	Data source
Subtropical coniferous forest	Jiangxi province, China	5.49	5.25	8.09	7.86	3.64	AGM	QYZ site
	Hunan province, China	-3.62	0.83	4.40	-0.40	5.93	AGM	HT site
Mature hardwood		–	–	10-330	–	2.23	MBR	
Yang pine plantation	Tennessee, USA	–	–	–	17-86	1.45	MBR	Lindberg et al. (1998) ^a
Boreal forest	Lake Gardsjon, Sweden	–	–	1-4	–	2.02	MBR	
Deciduous forest	Connecticut, USA	–	–	21.9	–	1.34	REA	Bash and Miller (2008) ^b
	Coventry Connecticut, England	–	–	-1.54	–	1.41	REA	Bash and Miller (2009)
Meadow	Fruebuel, central Switzerland	4.1	-4.8	2.5	0.3	1.29	AGM	Converse et al. (2010)
		-2.9	-1.5	3.2	-3.0	1.29	MBR	

599 ^a mean value (90% confidence interval), only measured during daytime;600 ^b median value of TGM (total gaseous mercury) flux

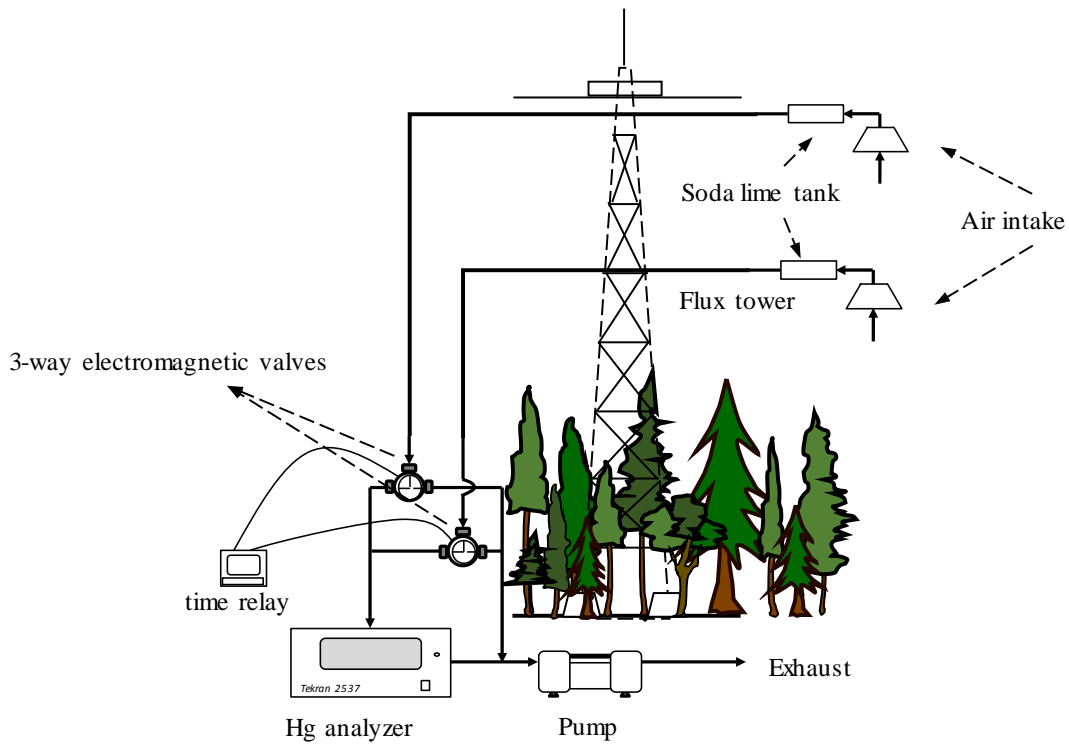
601



602

603 **Figure 1: Locations of the QYZ station, HT station and WS Mercury Mine. Vegetation map of China (CAS., 2007) as background.**

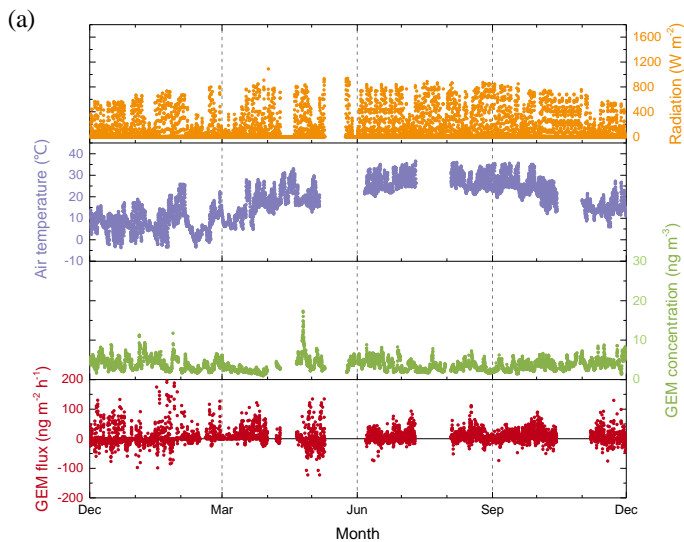
604



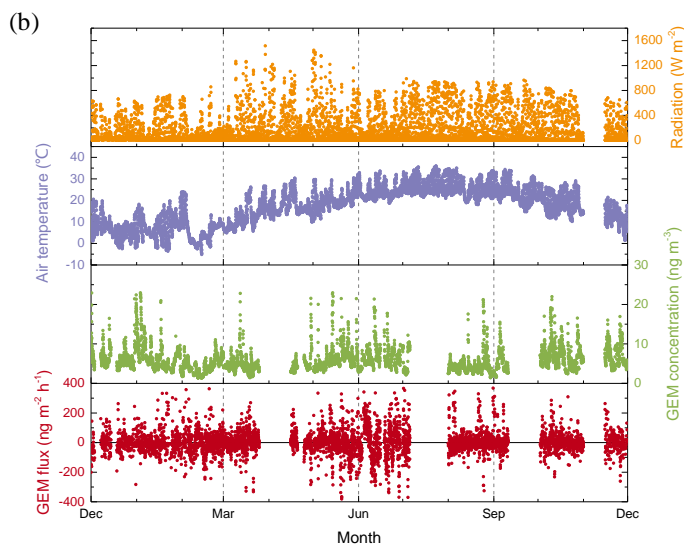
605

606 **Figure 2: Apparatus used to monitor vertical concentration gradient of GEM above forest canopy**

607



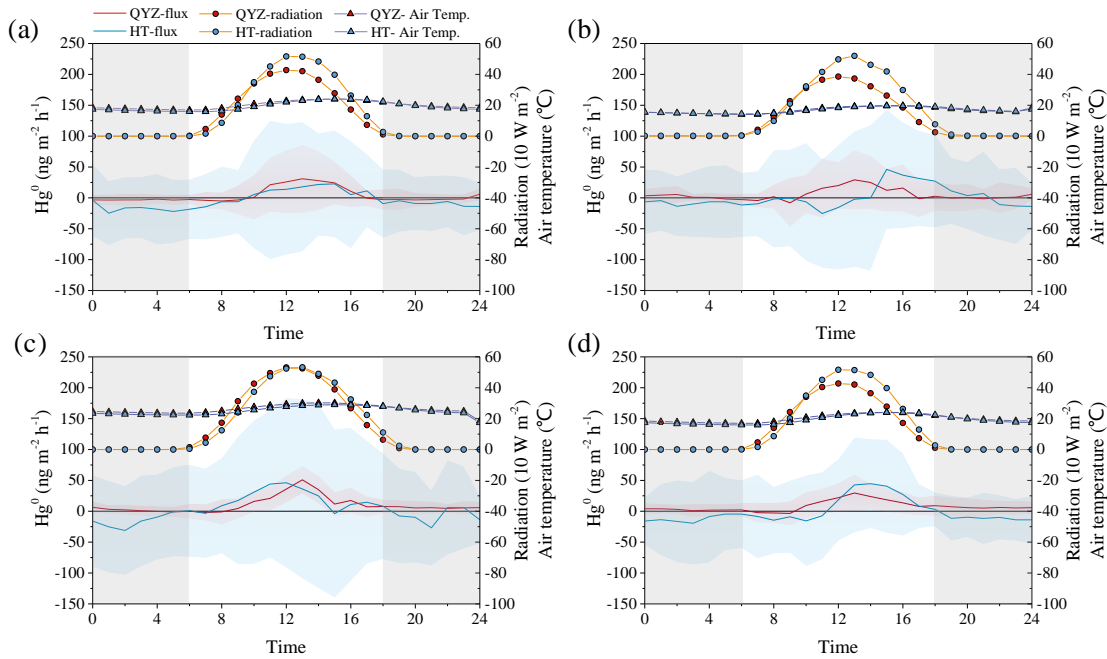
608



609

610

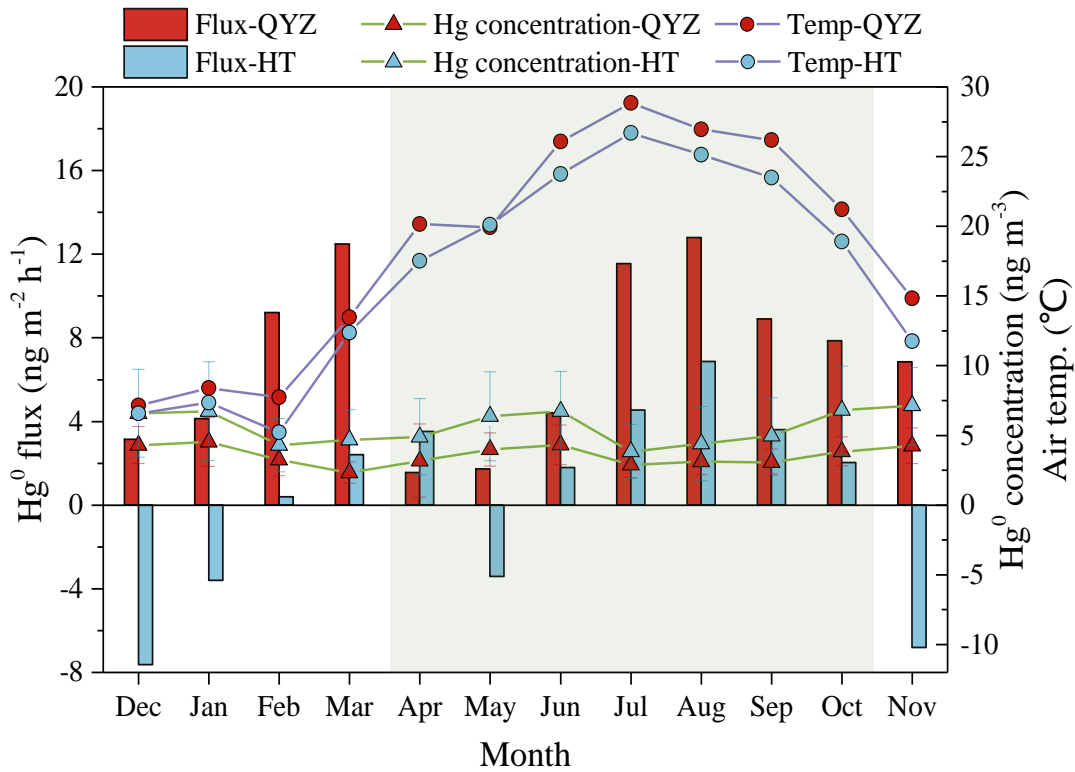
611 **Figure 3: Hourly-Annual variations of solar radiation, air temperature, GEM concentration (the average value of the GEM**
 612 **concentration at two heights), and GEM fluxes at QYZ (a) and HT (b) stations. The observations lasted for one year at both sites**
 613 **(January to December in 2014). The data in April, May and December was supplemented with the data in 2013 due to the use of**
 614 **mercury analyzer for measuring the soil and vegetation emission at HT site. Data loss were caused by elimination of the values**
 615 **outside the range of the monthly mean ± 3 standard deviations, and the problematic data during the high atmospheric stability,**
 616 **instrument failure and instability operation. The annual variations of GEM gradient and turbulent transfer coefficient (K) was**
 617 **showed in Figure S1.**



619

620 **Figure 4: Diurnal variation in GEM fluxes, air temperature and solar radiation over forest canopy in each season. (a) Winter:**621 **December to February; (b) Spring: March to May; (c) Summer: June to August; (d) Fall: September to October. Lines and**622 **envelopes depict mean values and standard variances. Diurnal variation in GEM gradient and turbulent transfer coefficient (K) in**
623 **each season at two sites was presented in Figure S2.**

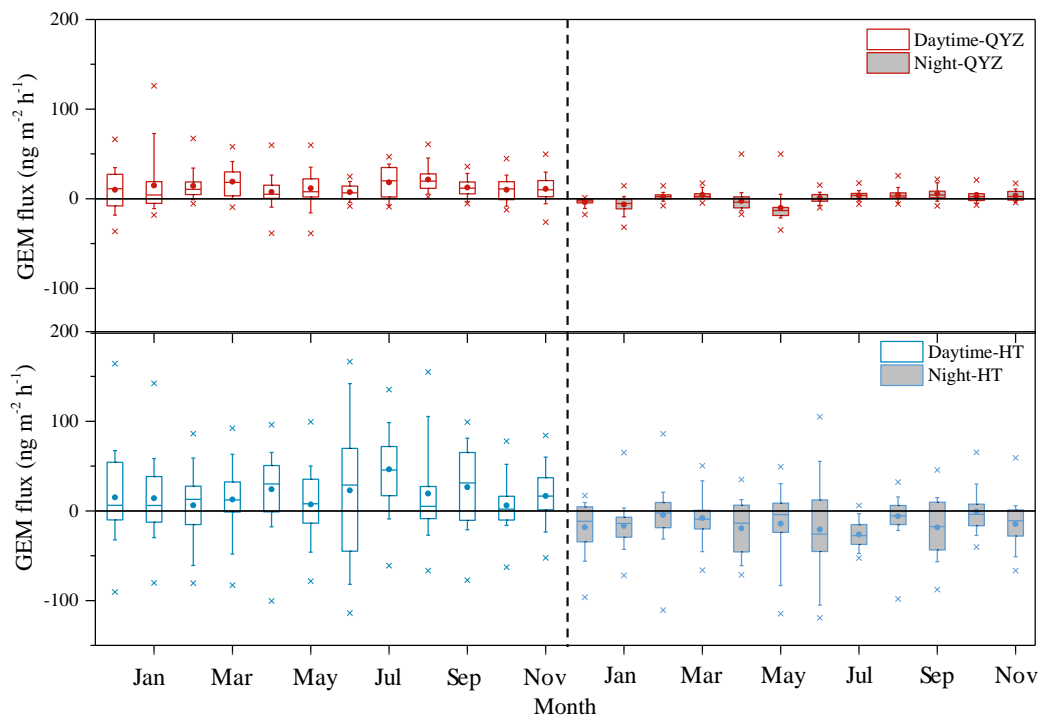
624



625

626 **Figure 5: Monthly variations of GEM flux, GEM concentration and air temperature at QYZ and HT sites. Leaf-growing season**
 627 **was marked as the shaded area.**

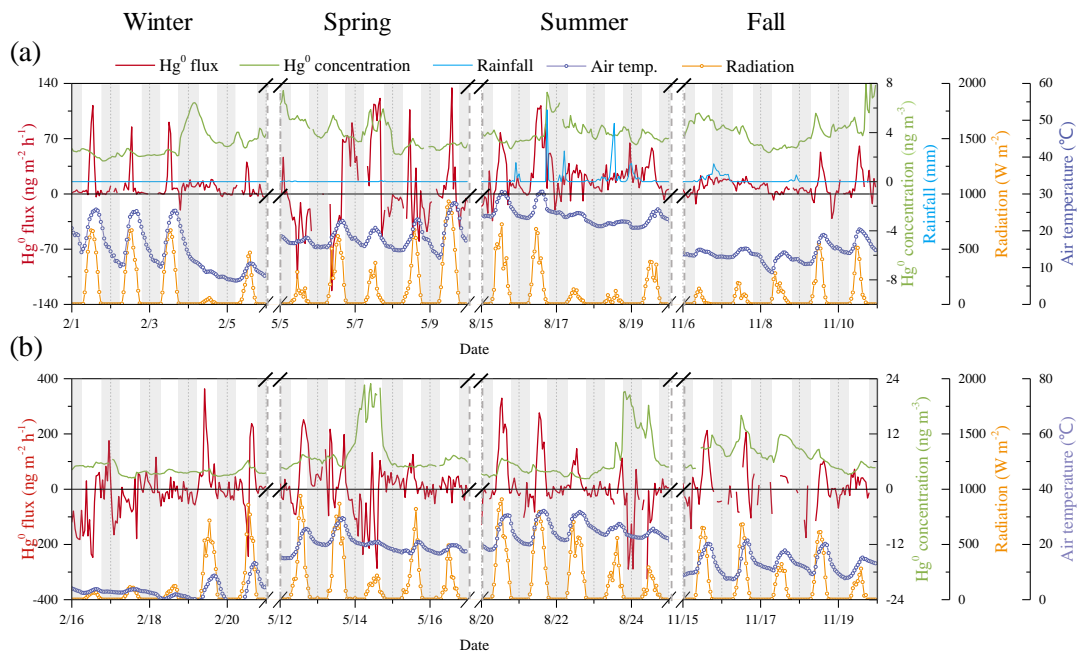
628



629

630 **Figure 6: Monthly variation in daytime GEM flux (upper panels) and night GEM flux (under panels) during the measurement**
 631 **periods at QYZ (a) and HT (b) sites. Box horizontal border lines represent the 25th, 50th and 75th percentiles from bottom to top,**
 632 **the whiskers include the 10th and 90th percentiles, and the outliers (cross) encompass the minimum and maximum percentiles. The**
 633 **solid circle in the box represents the mean value.**

634



635

636 **Figure 7: The GEM flux, concentration and environmental conditions in some typical days in each season at QYZ (a) and HT (b)**

637 **sites. Dates refer to China Standard Time (major ticks indicate midnight). All the data were indicated one-hour average.**

638